Electronic Supplementary Material (ESI) for Nanoscale.

Role of pre-nucleation clusters on the crystallization of gold nanoparticles

Raj Kumar Ramamoorthy,[1,2,3,*] Ezgi Yildirim,[1] Enguerrand Barba,[1] Pierre Roblin,[2] Jorge A. Vargas,[4,5] Lise-Marie Lacroix,[1] Isaac Rodriguez-Ruiz,[2] Philippe Decorse,[6] Valeri Petkov,[4] Sébastien Teychené,[2,*] Guillaume Viau[1,*]

[1] Université de Toulouse, Laboratoire de Physique et Chimie des Nano-Objets UMR 5215 INSA, CNRS, UPS, 135 avenue de Rangueil F-31077 Toulouse cedex 4, France

[2] Laboratoire de Génie Chimique, Université de Toulouse, CNRS, INP, UPS Toulouse, France

[3] Fédération de Recherche, Université de Toulouse, CNRS, INP, INSA, UPS, Toulouse France

[4] Department of Physics, Central Michigan University, Mt. Pleasant, MI-48858, USA

[5] Unidad Académica de Física, Universidad Autónoma de Zacatecas, Calz. Solidaridad esq. Paseo de la Bufa s/n, Zacatecas, Mexico

[6] Université de Paris, ITODYS UMR 7086, 15 rue Jean-Antoine de Baïf, 75013 Paris, France

SUPPLEMENTARY INFORMATIONS

Part 3. Characterizations of the nanoparticle precursors

Figure S5. X-ray absorption spectra at the Au L_{III}-edge of the Au(III) precursors with different OY concentrations ; Experimental real and imaginary components of the Fourier transform of the k^2-weighted EXAFS signal χ(k) and best fits.

Table S1. Molecular volume and electron density.

Figure S6. Fits of the SAXS pattern of the initial precursors obtained by dissolving $HAuCl_4$ in solution of OY in hexane : (a) [OY] = 50 mM ; (b) [OY] = 100 mM ; (c) [OY] = 400 mM.

Table S2. Fitted parameters to the SAXS pattern of the Au(III) precursors prepared with different OY concentration

Figure S7. *In situ* Au L_{III}-edge XAS of the Au(I) compound prepared by reaction of $HAuCl_4.3H_2O$ in pure oleyamine ; Experimental real and imaginary components of the Fourier transform of the k^2-weighted EXAFS signal χ(k) and best fits.

Part 4. *In situ* study of nucleation and growth of Au nanospheres

Scheme S2. Modelling of the reaction mechanism of the Au nanospheres formation with [OY] = 50 mM.

Table S3. Reaction rate constants of the different steps corresponding to the best fit of the gold speciation during the Au nanospheres formation with [OY] = 50 mM.

Figure S8. Kinetic modeling of the Au nanospheres synthesis with [OY] = 50 mM.

Figure S9. (a) Comparison of the SAXS pattern of the precursor and 4s after the introduction of TIPS. Examples of fits to experimental SAXS patterns with [OY] = 50 mM: (b) before the nucleation stage (t = 4 s); (c) after the nucleation stage (t = 288 s).

Table S4. Structural fit parameters of SAXS signals during the induction and the growth stages of the synthesis of gold nanospheres using [OY] = 50 mM.

Part 5. Influence of [OY] on kinetics of nucleation and growth

XAS spectra at the Au L_{III}-edge recorded as a function of time during the syntheses with [OY] = 100 mM and 400 mM

Figure S10. XAS spectra at the Au L_{III}-edge recorded as a function of time during the synthesis of Au nanoparticles by reduction of $HAuCl_4$ by TIPS in a solution of OY/hexane with [OY] = 100 mM and [OY] = 400 mM

Kinetic model for the nanowire synthesis with [OY] = 400 mM

Scheme S3. Modelling of the reaction mechanism of the Au nanowires formation with [OY] = 400 mM.

Table S5. Reaction rate constants of the different steps corresponding to the best fit of the gold speciation during the Au nanospheres formation with [OY] = 400 mM.

Figure S11. Kinetic modeling of the Au nanowires synthesis with [OY] = 400 mM.

Analysis of the SAXS patterns recorded during the nanosphere synthesis with [OY] = 100 mM

Figure S12. *In situ* time-resolved i*n situ* SAXS patterns recorded during the synthesis of Au nanoparticles with [OY] = 100 mM

Table S6. Structural fit parameters of SAXS signals during the induction and the growth stages of the synthesis of gold nanospheres using [OY] = 100 mM.

Part 1. Experimental set-up

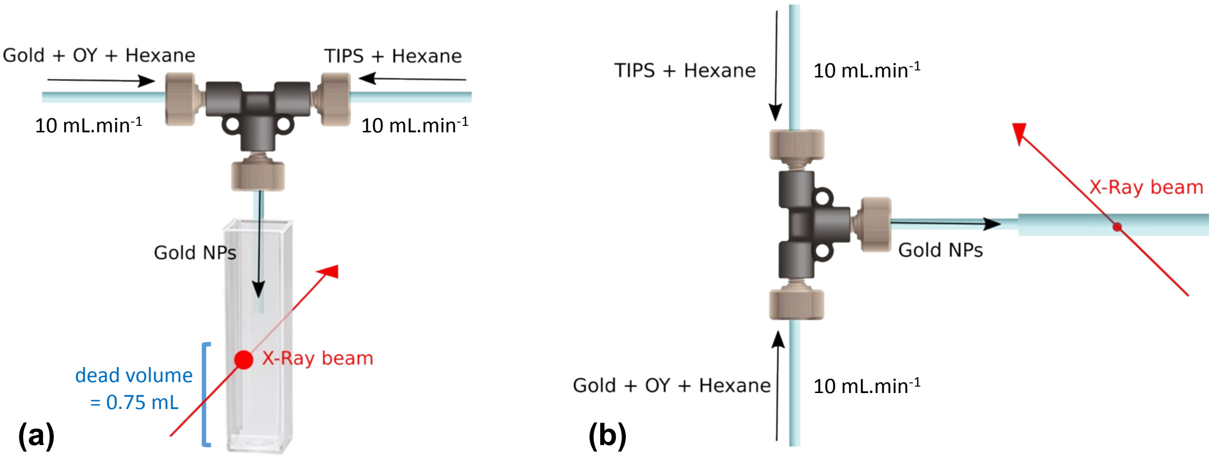

Scheme S1. Set-up used for XAS (a) and SAXS (b) experiments

Part 2. Additional nanoparticles characterizations

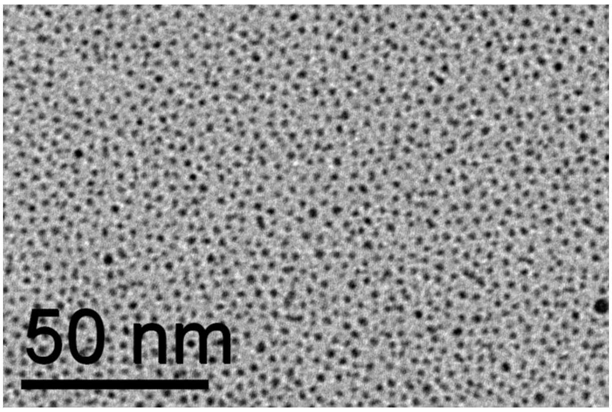

Figure S1. Transmission electron microscopy image of nanoparticles prepared by reduction of $HAuCl_4 \cdot 3H_2O$ in oleylamine solution in hexane, [OY] = 50 mM, reaction time = 24 h. The mean diameter of the particles is d_m = 2.2 nm, the standard deviation to the mean diameter is σ/d_m= 11 %.

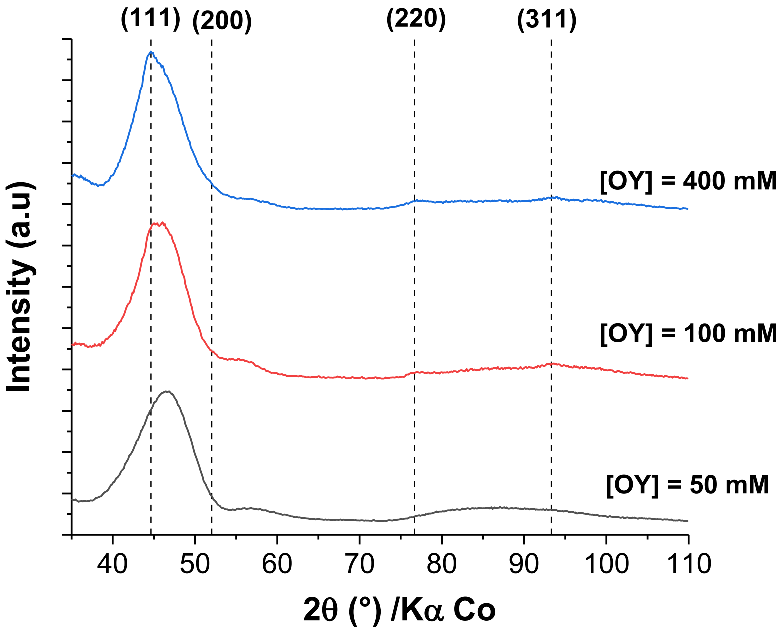

Figure S2. *Ex situ* XRD patterns of final nanoparticles prepared by reduction of $HAuCl_4.3H_2O$ dissolved in OY/hexane solutions at different OY concentrations with triisopropylsilane (TIPS) as reducing agent. In black : [OY] = 50 mM, recorded after a reaction of 3h; in red : [OY] = 100 mM recorded after a reaction of 3h; in blue : [OY] = 400 mM recorded after a reaction of 24 h.

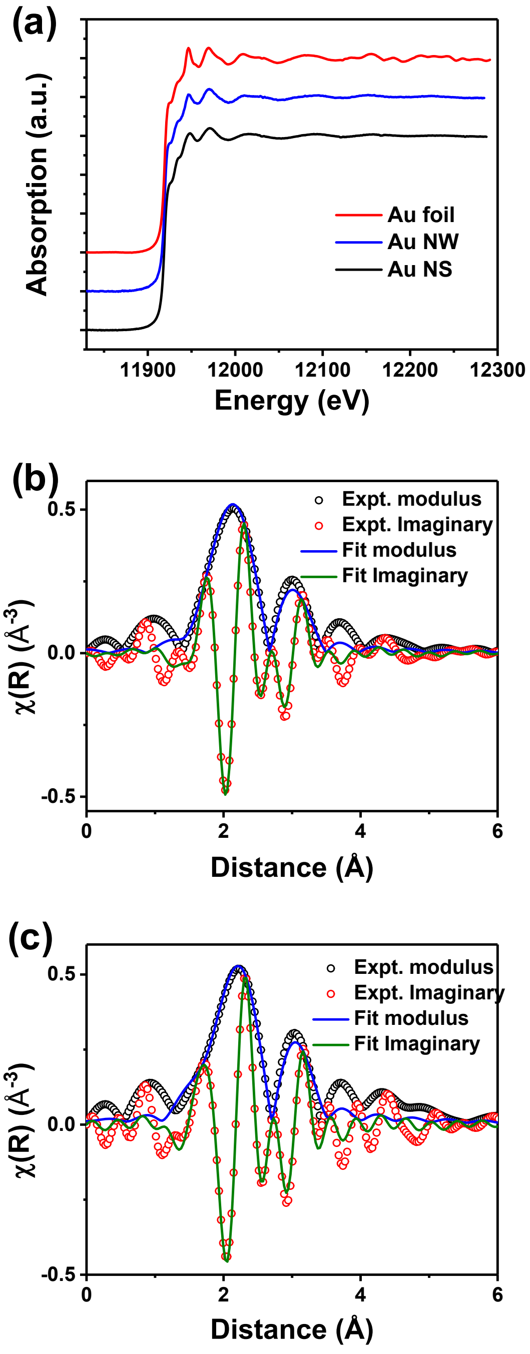

Figure S3. (a) *In situ* X-ray absorption spectra at the Au L_{III}-edge of Au nanoparticles prepared by reduction of $HAuCl_4.3H_2O$ in a solution of oleylamine in hexane using TIPS. Black line: Au NS stands for the nanospheres prepared with [OY] = 50 mM after 24 h of reaction; blue line: AuNW corresponds to the nanowires prepared with [OY] = 400 mM after 4 days of reaction; red line: gold foil as comparison. Experimental real and imaginary components of the Fourier transform of the k^2-weighted EXAFS signal $\chi(k)$ (open dots) and best fits (full lines) of Au NS (b) and Au NW (c). The reaction time

For the XAS spectra of the particles, the reaction times were intentionally extended to ensure that the reactions were complete and to avoid the presence of unreacted species, as these spectra were then used as references for the LCA analysis.

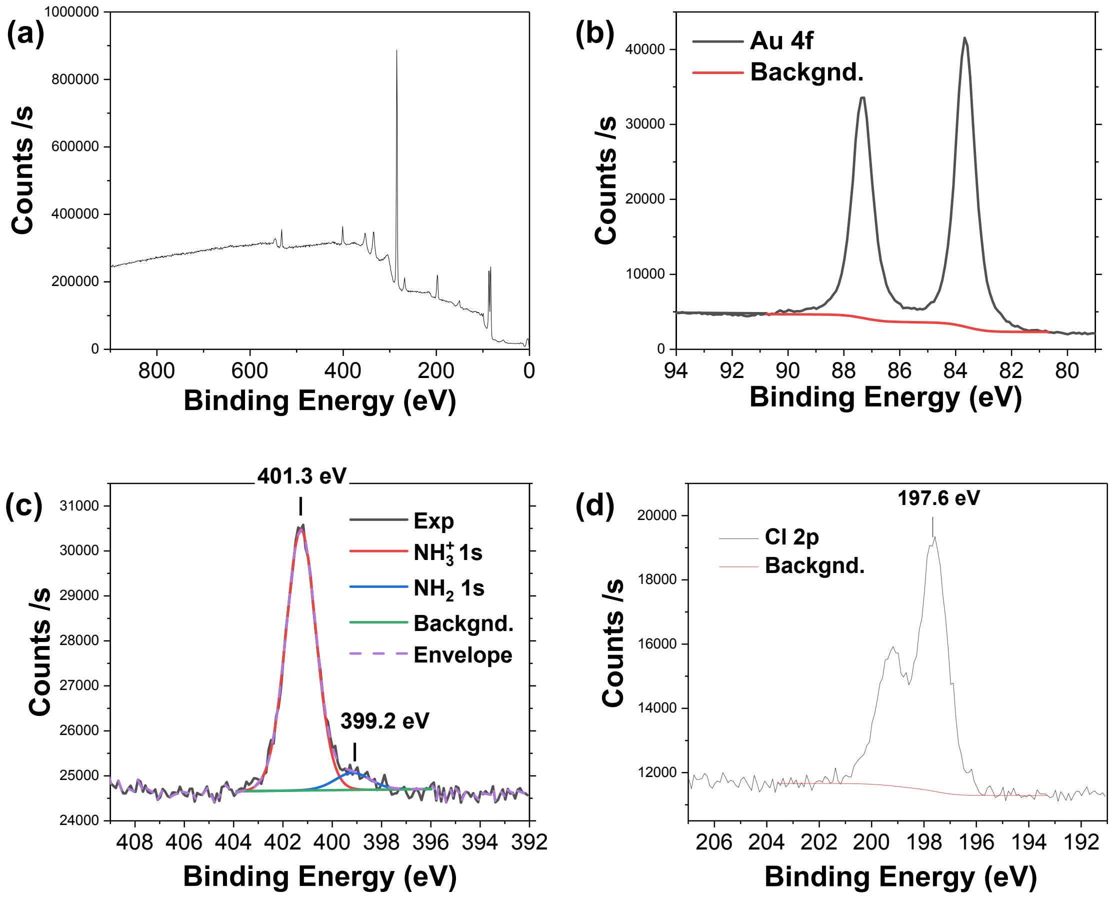

Figure S4. High resolution X-ray photon electron spectra of Au nanoparticles prepared with [OY] = 50 mM: (a) Survey scan; (b) Au 4f peak ; (c) N 1s peak showing a main contribution (93 %) at the binding energy of the ammonium cation (401.3 eV) and a minor contribution (7 %) at the binding energy of the amine (399.3 eV); (d) Cl 2p peak. The molar ratio Cl/N(ammonium) was found very close to 1 as expected for oleylammonium chloride.

Part 3. Characterizations of the nanoparticle precursors

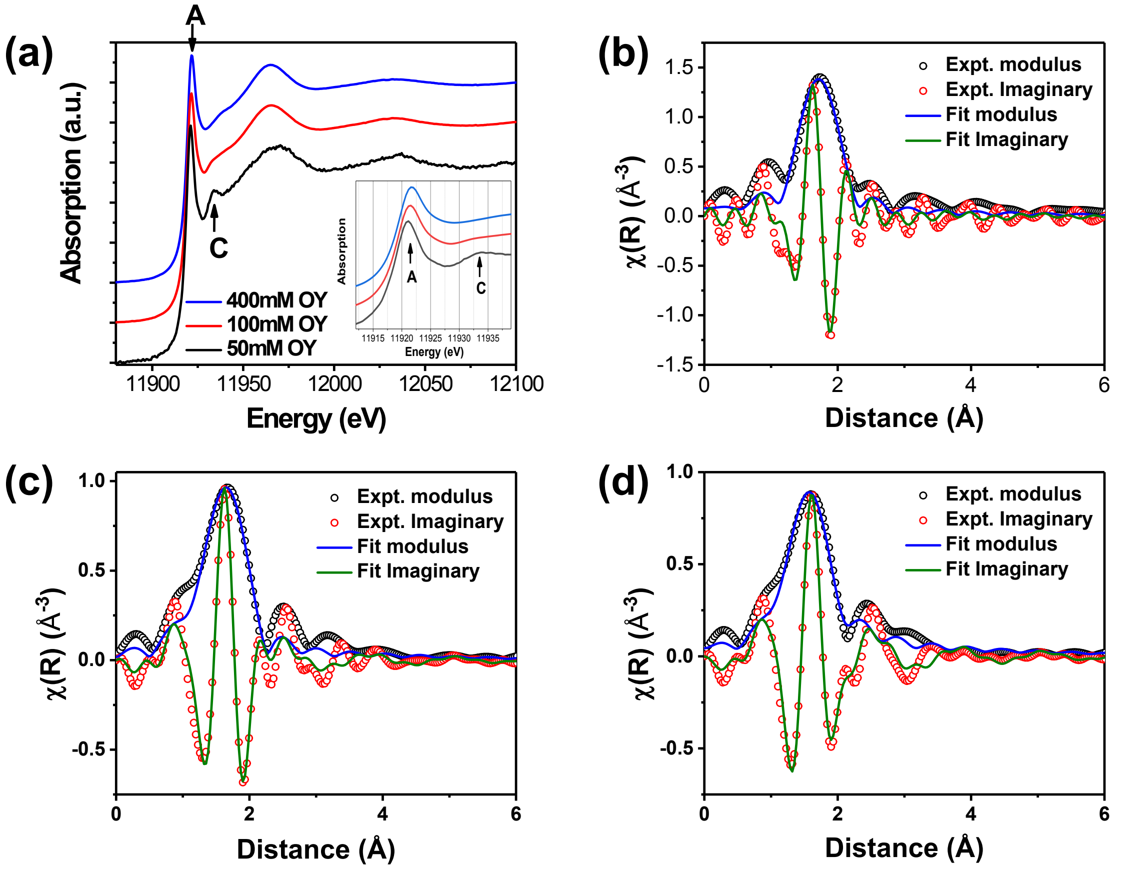

Figure S5. (a) *In situ* XAS spectra at the Au L_{III}-edge of $HAuCl_4$. $3H_2O$ ([Au] = 20 mM) in solution of oleylamine (OY) in hexane at different OY concentration (black: 50 mM; red: 100 mM; blue: 400 mM); Experimental real and imaginary components of the Fourier transform of the k^2-weighted EXAFS signal $\chi(k)$ (open dots) and best fits (full lines) for OY concentrations of (b) 50 mM ; (c) 100 mM ; (d) 400 mM.

Table S1. Molecular volume, V_m, and electron density (number of electron per unit volume), ρ^e, of the organic compounds used in the chemical synthesis, Au(III) and Au(I) reference compounds, and gold metal, the scattering length density (SLD), ρ, is the product of the electron density by the classical radius of the electron $r_e = 2.81794 \times 10^{-15}$ m.

Name	Molecular formula	V_m (nm^3)	ρ^e (e.nm^{-3})
Hexane	C_6H_{14}		230 [a]
Oleylamine (OY)	$C_{18}H_{37}N$	0.545	280 [a]
Triisopropylsilane (TIPS)	$C_9H_{22}Si$		266 [a]
Amine Au(III) trichloride	$AuCl_3NH_3$	0.134	1047 [b,1]
Sodium Au(III) tetrachloride	$AuCl_4Na$	0.161	983 [b,2]
Au(I) chloride	AuCl	0.049	1954 [b,3]
$TBA^+[Au(III)Cl_4]^-$	$C_{16}H_{36}N_4AuCl_4$	0.563	508 [b,4]
$OY^+[Au(III)Cl_4]^-$	$C_{18}H_{38}NAuCl_4$	0.679	442 [c]
$OY\text{-}Au(III)Cl_3$	$C_{18}H_{37}NAuCl_3$	0.679	415 [c]
OY-Au(I)Cl	$C_{18}H_{37}NAuCl$	0.594	417 [c]
Gold metal	Au(0)		4650 [b]

[a] values calculated from the molar mass and density; [b] values calculated from the crystallographic structure of the solid; [c] values estimated from the molar volume of oleylamine and $AuCl_3NH_3$ or AuCl.

---

[1] J. Strähle, J. Gelinek, M. Kölmel, *Z. anorg. allg. Chem.* **1979**, *466*, 241- 260.

[2] P. G. Jones, R. Hohbein, E. Schwarzmann, *Acta Cryst. C*, **1988**, *44*, 1166-1168.

[3] E. M. W. Janssen, J. C. W. Folmer, G. A. Wiegers, *J. Less Common Met.*, **1974**, *38*, 71-76.

[4] R. W. Buckley, P. C. Healy, W. A. Loughlin, *Aust. J. Chem.* **1997**, 50, 775-778 ; C.J. Serpell, J. Cookson, D. Ozkaya, P. D. Beer, *Nat. Chem.* **2011**, *3*, 478-483.

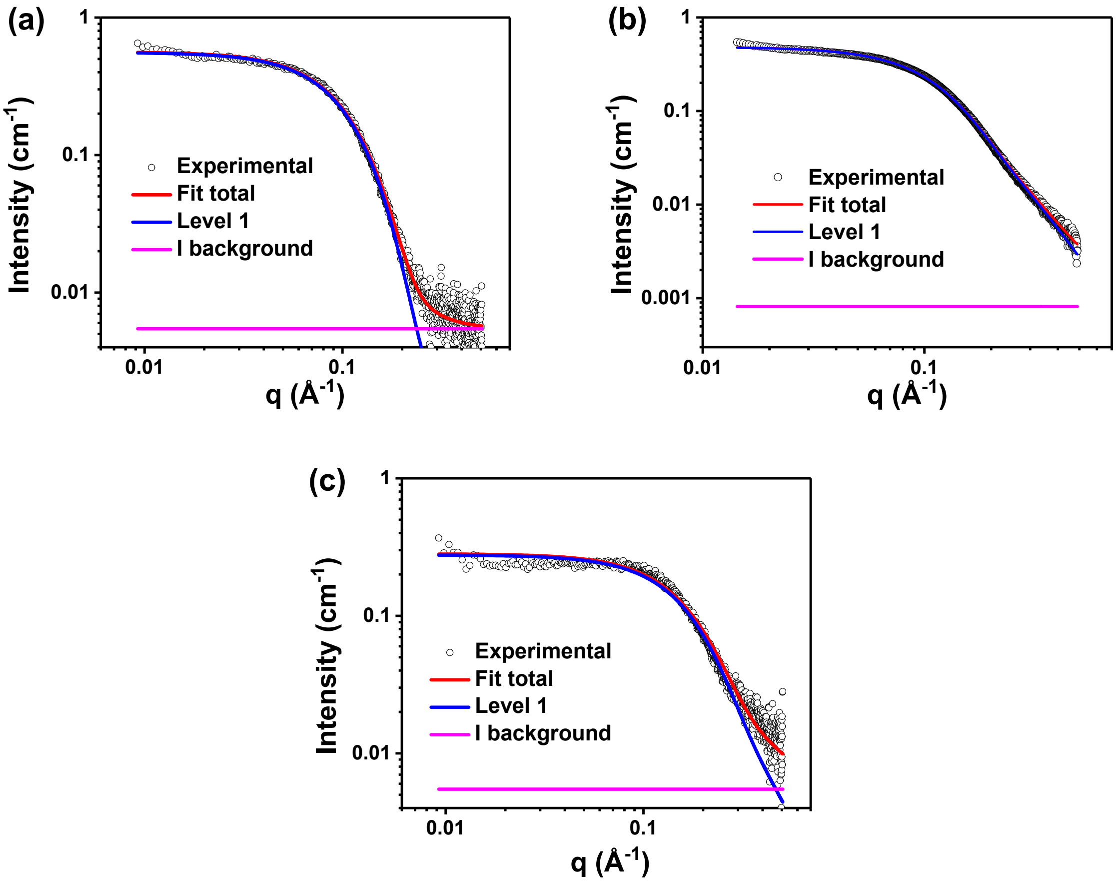

Figure S6. Fits of the SAXS pattern of the initial precursors obtained by dissolving $HAuCl_4$ in solution of OY in hexane : (a) [OY] = 50 mM ; (b) [OY] = 100 mM ; (c) [OY] = 400 mM. A single level Beaucage equation[5] was fitted to the SAXS patterns of the precursors:

$$I(q) = Gexp\left(-\frac{q^2R_g^2}{3}\right) + B\left(\frac{1}{q}\right)^p + I_{bg}(q) \qquad \text{(Eq. S1)}$$

The radius of gyration, R_g, and the slope of the power law given by the best fitting are reported in table S2.

Table S2. Fitted parameters to the SAXS pattern of the Au(III) precursors prepared with different OY concentration. R_g is the gyration radius, D_{SAXS} the diameter of the objects calculated from the gyration radius assuming a spherical shape, $D_{SAXS} = 2\sqrt{5/3}R_g$, and p is the slope of the power law in the high-q region (Porod regime).

Au(III) precursor	R_g (Å)	D_{SAXS} (nm)	p
[OY] = 50 mM	17.1	4.4	3.5
[OY] = 100 mM	15.1	3.9	3.1
[OY] = 400 mM	10.4	2.7	2.8

---

[5] G. Beaucage, *J. Appl. Cryst.* **1996**, *29*, 134-146.

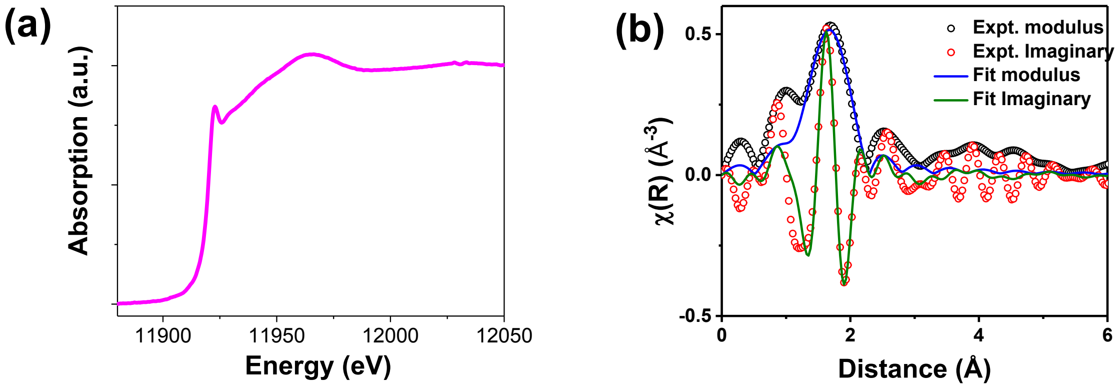

Figure S7. (a) *In situ* Au L_{III}-edge XAS of the Au(I) compound prepared by reaction of $HAuCl_4.3H_2O$ in pure oleyamine for 48 h; (b) Experimental real and imaginary components of the Fourier transform of the k^2-weighted EXAFS signal χ(k) (open dots) and best fits (full lines). This spectrum was introduced a possible Au(I) contribution to the LCA of the time-resolved XAS spectra with the XAS spectra of the Au(III) precursors (Fig. S5a) and final Au(0) nanoparticles (Fig. S3a).

Part 4. *In situ* study of nucleation and growth of Au nanospheres with [OY] = 50 mM

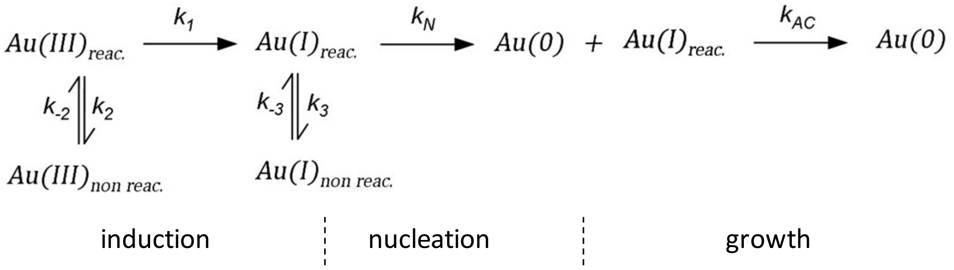

Scheme S2. Modelling of the reaction mechanism of the Au nanospheres formation with [OY] = 50 mM. The reduction pathway involves a two-step reaction, Au(III) to Au(I) and Au(I) to Au(0). The Au(0) NP nucleation/growth process is modelled by an auto-catalytic process with the reaction rate constants k_N and k_{AC}. A competition between reduction and complexation of the Au(III) and Au(I) by OY is described by two additional equilibrium during the induction stage. The two "non reactive" complexes are not directly involved in the reduction steps but act as reservoir for the "reactive complexes".

Only first order reactions have been considered for the sake of simplification. Nevertheless, for the reaction involving TIPS, reduction of Au(III) to Au(I) and Au(I) to Au(0), the reduction of the reaction order is justified insofar as TIPS is always in a very large excess, therefore its concentration is constant throughout the reaction and does not modify the rates of the reduction steps. For the reaction involving OY, the assumption of first order reaction may be a rough approximation.

The concentrations of the 5 species involved in the reaction were calculated solving numerically the set of differential equations given below and fitting the concentrations $[Au(III)_T] = [Au(III)_R] + [Au(III)_{NR}]$, $[Au(I)_T] = [Au(I)_R] + [Au(I)_{NR}]$ and $[Au(0)] = 1 - [Au(III)_T] - [Au(I)_T]$ to the experimental curves obtained from the LCA of the XAS signals. The numerical integration of the ordinary differential equations and nonlinear fittings were performed with the functions ODE15s and LSQNONLIN of MATLAB, respectively.

$$\frac{d[Au(III)_R]}{dt} = -(k_1 + k_2) \times [Au(III)_R] + k_{-2}[Au(III)_{NR}]$$

$$\frac{d[Au(III)_{NR}]}{dt} = k_2 \times [Au(III)_R] - k_{-2} \times [Au(III)_{NR}]$$

$$\frac{d[Au(I)_{NR}]}{dt} = k_3 \times [Au(I)_R] - k_{-3} \times [Au(I)_{NR}]$$

$$\frac{d[Au(I)_R]}{dt} = k_1 \times [Au(III)_R] - k_3 \times [Au(I)_R] + k_{-3} \times [Au(I)_{NR}] - k_N \times [Au(I)_R] - k_{AC} \times [Au(I)_R][Au(0)]$$

Figure S8(a,b) depicts the comparison between the experimental gold speciation and the best fitting curves given by this model. The fitted reaction rate constants are reported in Table S3. The constants relative to the reduction rate, k_1 and k_N, are higher than the rate constants relative to the formation of the non-reactive species, k_2 and k_3. Nevertheless, the high values of the two equilibrium constants, $K_2 = k_2/k_{-2} = 16.7$ and $K_3 = k_3/k_{-3} = 48$, make possible the formation of reservoirs of non-reactive species. Their transformation into reactive species are the limiting steps of the reaction during the growth stage. The nucleation rate, $V_{Nucleation} = k_N[Au(I)_R]$, the growth rate, $V_{growth} = k_{AC}[Au(I)_R][Au(0)]$, and the ratio $\frac{V_{growth}}{V_{Nucleation}}$ calculated from the model are plotted as a function of time in Figure S8(c,d). The maximum of the nucleation rate is reached at the maximum of the reactive Au(I) specie concentration: $v_{N\,max} = k_N[Au(I)_R]_{max} = 0.495\ min^{-1} = 8.25\ 10^{-3}s^{-1}$. The figure S8c shows an overlap between the nucleation and growth stages. According to the rate constants reported in Table S3, $V_{growth} > V_{Nucleation}$ for t > 22s and $V_{growth} > 2V_{Nucleation}$ for t > 40 s (FIg. S8d).

Table S3. Reaction rate constants of the different steps corresponding to the best fit of the gold speciation during the Au nanospheres formation with [OY] = 50 mM.

Constant	k_1	k_2	k_{-2}	k_3	k_{-3}	k_N	k_{AC}
Value (min^{-1})	2.16	0.996	0.0596	1.269	0.0263	2.296	11.18
Value (s^{-1})	$3.60\ 10^{-2}$	$1.66\ 10^{-2}$	$9.93\ 10^{-4}$	$2.12\ 10^{-2}$	$4.39\ 10^{-4}$	$3.83\ 10^{-2}$	$1.86\ 10^{-1}$

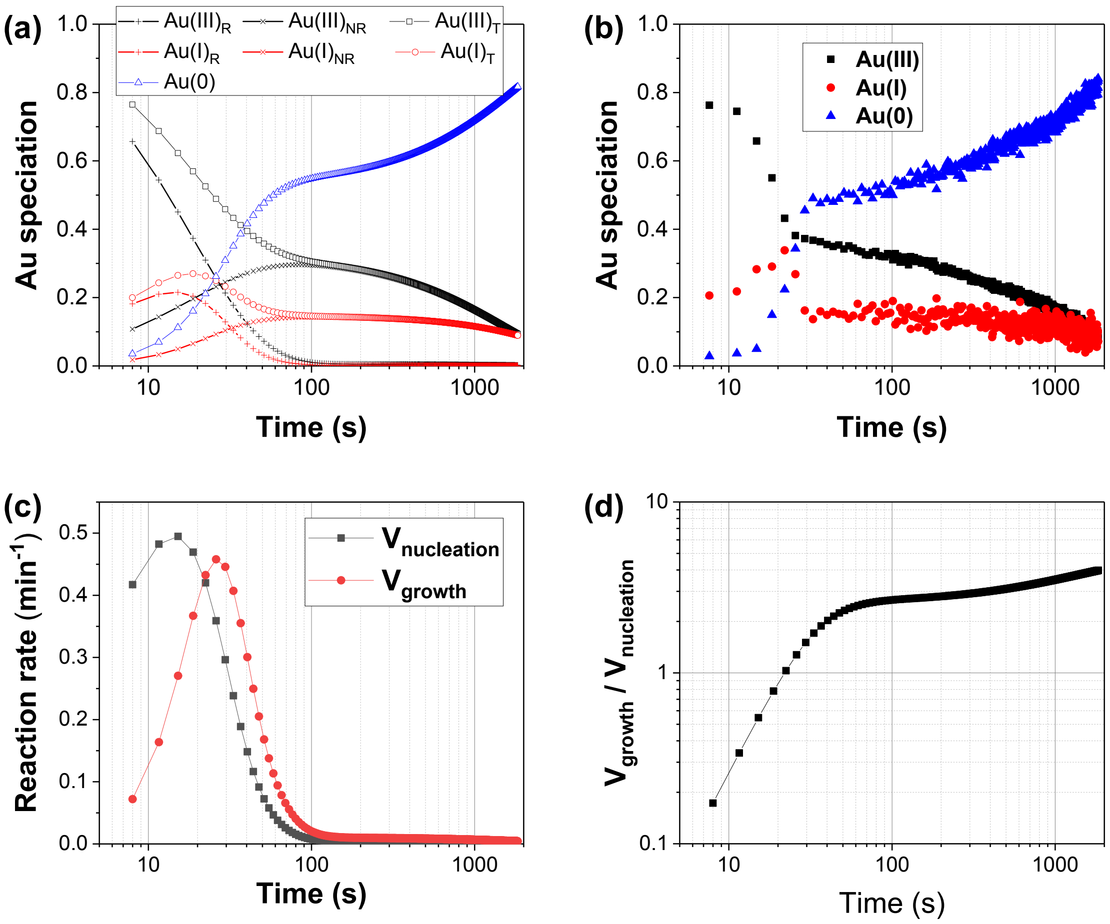

Figure S8. Kinetic modeling of the Au nanospheres synthesis with [OY] = 50 mM. (a) Time evolution of the Au(III) and Au(I), reactive (R) and non reactive (NR) species, total (T) Au(III), Au(I) and Au(0) relative concentrations, given by the best fit to the experimental gold speciation; (b) Experimental gold speciation; (c) Nucleation and growth rates given by the fit; (d) Ratio between the growth and nucleation rates as a function of time.

Analysis of the SAXS patterns recorded during the nanosphere synthesis with [OY] = 50 mM

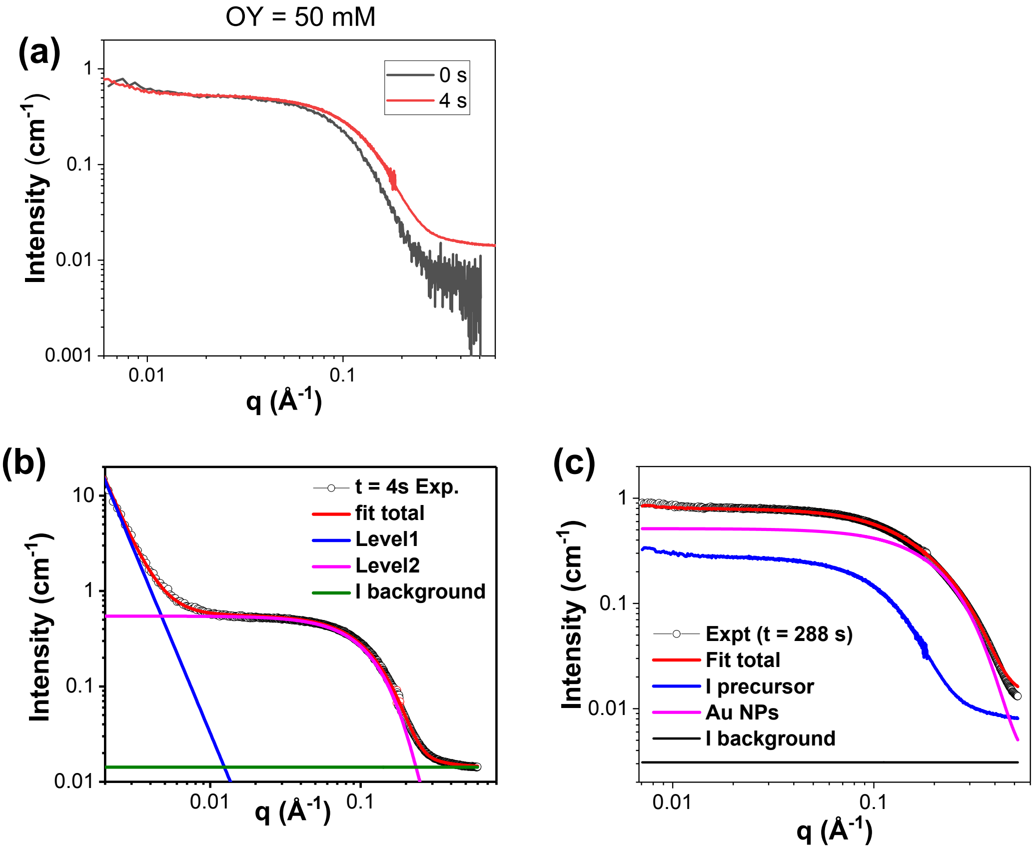

Figure S9. (a) Comparison of the SAXS pattern of the precursor and 4s after the introduction of TIPS**.** Examples of fits to experimental SAXS patterns with [OY] = 50 mM: (b) before the nucleation stage (t = 4 s); (c) after the nucleation stage (t = 288 s).

The SAXS patterns were analyzed as follow:

Before the nucleation stage, the scattering intensity was interpreted by the presence of pre-nucleation clusters, responsible for the intensity at high- and intermediate-q ranges, these substructure units being assembled into larger structures responsible for the low-q power law.

the SAXS curves were fitted to a two structural level Beaucage equation[1]:

$$I(q) = G_1 exp\left(-\frac{q^2 R_{g(1)}^{2}}{3}\right) + B_1 exp\left(-\frac{q^2 R_{g(2)}^{2}}{3}\right)\left(\frac{1}{q_1^*}\right)^{p_1} + G_2 exp\left(-\frac{q^2 R_{g(2)}^{2}}{3}\right) + B_2\left(\frac{1}{q_2^*}\right)^{p_2} + I_{bg}(q)$$

(Eq. S2)

where $q_i^* = q/\left[erf\left(qR_{g(i)}/\sqrt{6}\right)\right]^3$, G_i and B_i are the prefactors for the Guinier and the power law scattering regions, respectively, p_i refers to the exponent corresponding to decay of scattering signal in the power law regions, R_{g1} and R_{g2} are the radius of gyration of the largest and smallest structures, respectively, and $I_{bg}(q)$ refers to a background function corresponding to the incoherent scattering contribution. In our case, the Guinier region for the largest structures was out of the accessible q range. The first term of Eq. S2 was not considered. The following terms of Eq. S2 describe the power law regime at low-q, the Guinier regime in the intermediate-q range and the power law at high-q. The fitted parameters to the experimental SAXS were B_1, G_2, B_2, p_1, p_2, R_{g2} and the background function $I_{bg}(q)$.

<u>After the nucleation stage</u>, the SAXS curves varied mainly in the intermediate and high-q ranges, resulting from an increasing contribution of Au nanoparticles and a decreasing contribution of the pre-nucleation clusters. The total scattering intensity was fitted to a sum of three contributions:

$$I(q) = \alpha \times I_{prec.}(q) + I_{NP}(q) + I_{bg}(q) \qquad \text{(Eq. S3)}$$

with $I_{prec.}(q)$ the scattering intensity of the remaining precursors and α the weight of the precursor contribution, $I_{NP}(q)$ the scattering intensity of the metal nanoparticles and $I_{bg}(q)$ the background function corresponding to the incoherent scattering contribution. The scattering intensity at t = 22s, i.e. at the end of the induction stage, was taken as reference for the remaining precursor contribution. A single level Beaucage equation was used for the nanoparticle contribution :

$$I_{NP}(q) = G_{NP} exp\left(-\frac{q^2 R_g^2}{3}\right) + B_{NP}\left(\frac{1}{q}\right)^p + I_{bg}(q) \qquad \text{(Eq. S4)}$$

The fitting parameters, G_{NP}, R_g, B_{NP}, p take the same meaning as above.

Table S4. Structural fit parameters of SAXS signals during the induction and the growth stages of the synthesis of gold nanospheres using [OY] = 50 mM, using Beaucage model. R_g is the gyration radius, D_{SAXS} the diameter of the objects calculated from the gyration radius assuming a spherical shape, p_i the exponents of the Porod region, p_1 refers to the low-q region and p_2 to the high-q region. α is the relative weight of the pre-nucleation clusters (PNCs) used to fit the growth stage (α = 1 at 22s).

Time	Pre-nucleation clusters Induction stage			Secondary aggregates
	R_g (Å)	D_{SAXS} (nm)	P_2	P_1
0 s	17.1(1)	4.4(2)	3.5(1)	-
2 s	16.5(1)	4.2(2)	3.5(1)	3.6(1)
4 s	14.9(1)	3.8(2)	3.2(1)	3.8(1)
10 s	14.8(1)	3.8(2)	3.1(1)	3.7(1)
22 s	15(1)	3.9(2)	3.4(1)	3.5(1)
Time	Metal Nanoparticles Growth stage			Relative weight of PNCs
	R_g (Å)	D_{SAXS} (nm)	P_2	α
36 s	7.5(1)	1.9(2)	3.7(3)	0.67

48 s	7.6(1)	2.0(2)	3.7(3)	0.65
88 s	7.7(1)	2.0(2)	3.7(3)	0.61
288 s	8(1)	2.1(2)	3.7(3)	0.51
488 s	8.4(1)	2.2(2)	3.7(3)	0.47
688 s	8.8(1)	2.3(2)	3.7(3)	0.37
1088 s	9.4(1)	2.4(2)	3.7(3)	0.34
1706 s	9.4(1)	2.4(2)	3.7(3)	0.24

Part 5. Influence of [OY] on kinetics of nucleation and growth

XAS spectra at the Au L_{III}-edge recorded as a function of time during the syntheses with [OY] = 100 mM and 400 mM

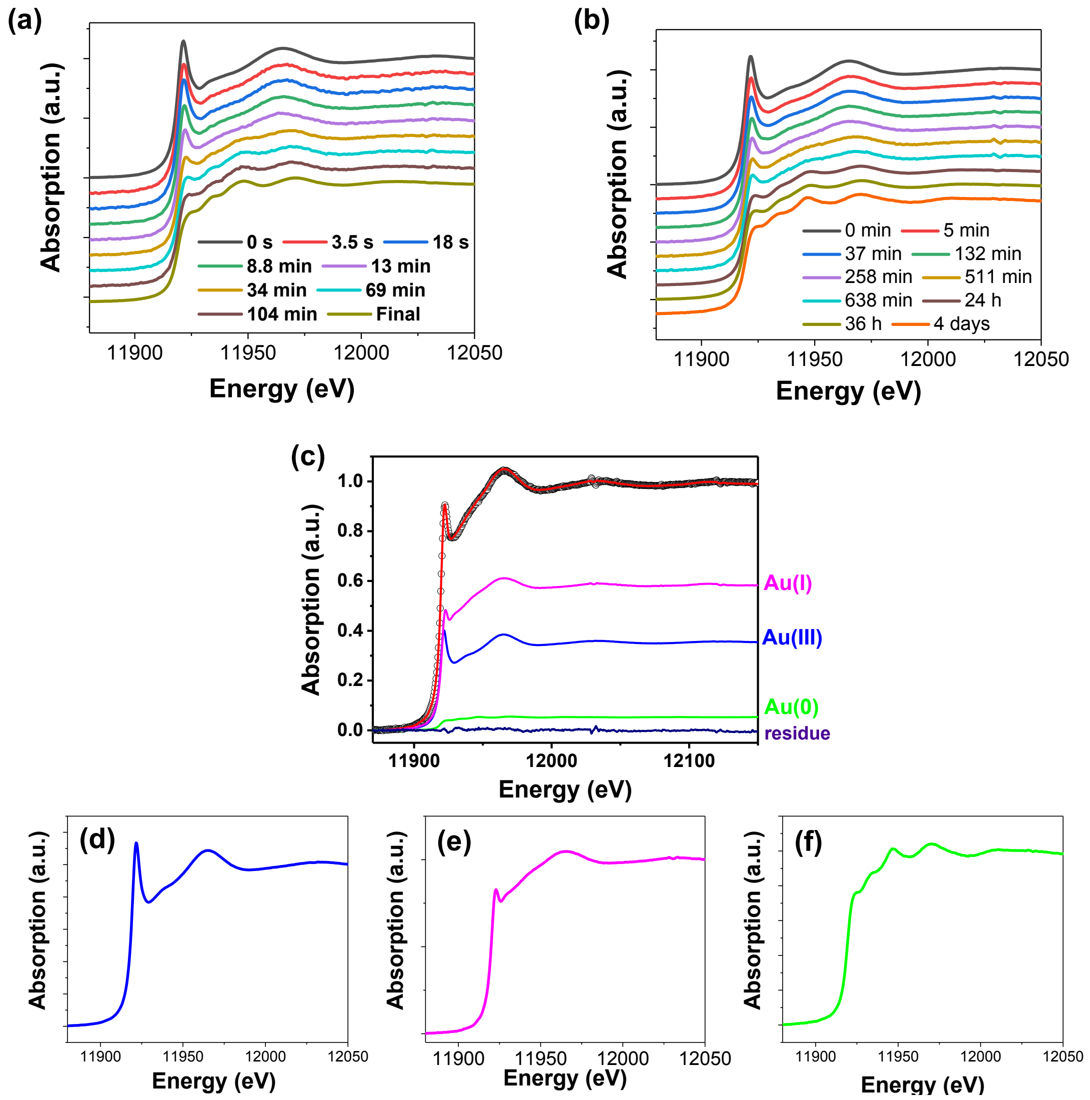

Figure S10. XAS spectra at the Au L_{III}-edge recorded as a function of time during the synthesis of Au nanoparticles by reduction of $HAuCl_4$ by TIPS in a solution of OY/hexane with (a) [OY] = 100 mM and

(b) [OY] = 400 mM; (c) Example of fit of a linear combination (red line) to an experimental XAS spectrum (open circles) with [OY] = 400 mM at t = 258 min. The 3 components of the LCA are the XAS spectrum of $HAuCl_4$ just after its dissolution in the solution of OY in hexane (d) already shown in figure S5a, the lamellar phase prepared by the reaction of $HAuCl_4$ in pure oleylamine (e) already shown in figure S7; the final Au nanowires (f) already shown in figure S3a.

Kinetic model for the nanowire synthesis with [OY] = 400 mM

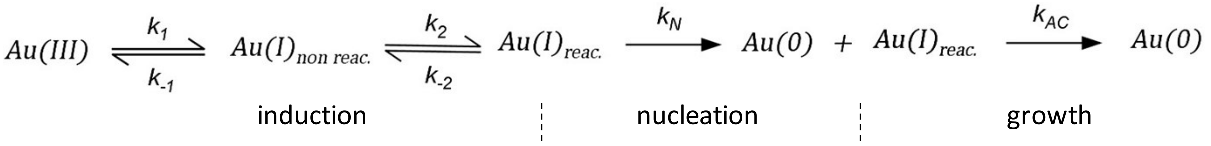

Scheme S3. Modelling of the reaction mechanism of the Au nanowires formation with [OY] = 400 mM. The Au(0) NP nucleation/growth process is modelled by an auto-catalytic process with the reaction rate constants k_N and k_{AC}. The very large excess of oleylamine in the medium favors the formation of a “non-reactive” Au(III) complex. This complex is progressively reduced into a “non-reactive” Au(I) complex in equilibrium with a reactive Au(I) complex which is finally involved in the Au(0) formation. Both “non reactive” complexes serve as reservoir for the “reactive complexes”.

As in the previous model, only first order reactions have been considered for the sake of simplification. In these experimental conditions, both TIPS and OY are in large excess compared to gold. Thus, the reduction of the order of reaction is justified for all the reactions involving TIPS or OY. Their concentration can be considered as almost constant throughout the reaction.

The concentrations of the 4 species involved in the reaction were calculated solving numerically the set of differential equations given below and fitting the concentrations $[Au(III)_T] = [Au(III)_R] + [Au(III)_{NR}]$, $[Au(I)_T] = [Au(I)_R] + [Au(I)_{NR}]$ and $[Au(0)] = 1 - [Au(III)_T] - [Au(I)_T]$ to the experimental curves obtained from the LCA of the XAS signals. The numerical integration of the ordinary differential equations and nonlinear fittings were performed with the functions ODE15s and LSQNONLIN of MATLAB, respectively.

$$\frac{d[Au(III)]}{dt} =- k_1 \times [Au(III)] + k_{-1}[Au(I)_{NR}]$$

$$\frac{d[Au(I)_{NR}]}{dt} = k_1 \times [Au(III)] - k_{-1}[Au(I)_{NR}] - k_2 \times [Au(I)_{NR}] + k_{-2} \times [Au(I)_R]$$

$$\frac{d[Au(I)_R]}{dt} = + k_2 \times [Au(I)_{NR}] - k_{-2} \times [Au(I)_R] - k_N \times [Au(I)_R] - k_{AC} \times [Au(I)_R][Au(0)]$$

Figure S10(a,b) depicts the comparison between the experimental gold speciation and the best fitting curves given by this model. The fitted reaction rate constants are reported in Table S4. All the reaction rate constants are much smaller than in the case of [OY] = 50 mM. The nucleation and auto-catalytic rate constants, in particular, are 3 orders of magnitude lower with [OY] = 400 mM compared to [OY] =

50 mM. The nucleation and growth rates calculated from the model are plotted as a function of time in Figure S10c. The maximum of the nucleation rate is reached for the maximum of the reactive Au(I) specie concentration: $v_{N\,max} = k_N[Au(I)_R]_{max} = 1.57\ 10^{-4}\,min^{-1} = 2.6\,10^{-6}\,s^{-1}$. However, the main difference with the previous case ([OY] = 50 mM) is that the growth rate becomes higher than the nucleation rate before this last one has reached its maximum value. The ratio between the growth rate and the nucleation rate is given by $\frac{V_{growth}}{V_{Nucleation}} = \frac{k_{AC}}{k_N}[Au(0)]$. The ratio $\frac{k_{AC}}{k_N}$ is much higher for [OY] = 400 mM than for [OY] = 50 mM, as a result V_{growth} increases much faster than $V_{Nucleation}$ and reaches much higher values. The overlap between the nucleation and growth stage is less extended than in the case of the nanospheres. According to the rate constants reported in Table S4, $V_{growth} > V_{Nucleation}$ for t > 155 min and $V_{growth} > 2V_{Nucleation}$ for t > 200 min (FIg. S10d). Interestingly, the relative amount of Au(0) produced fir these times are 1.5 and 2.5 %. The model describes well that the nucleation stage involves only a very small amount of gold, at the opposite of the kinetic of the nanospheres with [OY]= 50 mM.

Table S5. Reaction rate constants of the different steps corresponding to the best fit of the gold speciation during the Au nanospheres formation with [OY] = 400 mM.

Constant	k_1	k_{-1}	k_2	k_{-2}	k_N	k_{AC}
Value (min^{-1})	$6.41\ 10^{-3}$	$3.81\ 10^{-3}$	$2.14\ 10^{-3}$	$1.50\ 10^{-3}$	$1.23\ 10^{-3}$	$9.05\ 10^{-2}$
Value (s^{-1})	$1.07\ 10^{-4}$	$6.36\ 10^{-5}$	$3.57\ 10^{-5}$	$2.49\ 10^{-5}$	$2.05\ 10^{-5}$	$1.51\ 10^{-4}$

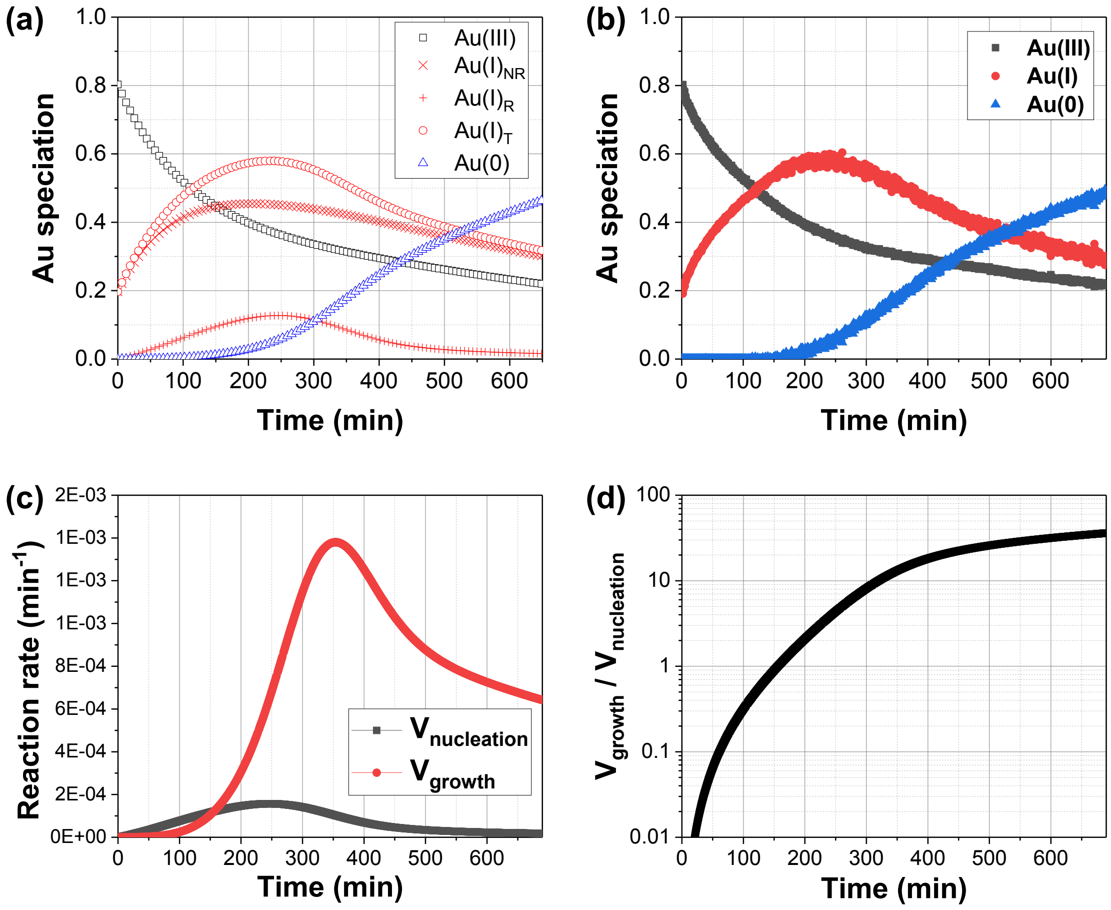

Figure S11. Kinetic modeling of the Au nanowires synthesis with [OY] = 400 mM. (a) Time evolution of the Au(III) and Au(I), reactive (R) and non-reactive (NR) species, total (T) Au(III), Au(I) and Au(0) relative concentrations, given by the best fit to the experimental gold speciation; (b) Experimental gold speciation; (c) Nucleation and growth rates given by the fit; (d) Ratio between the growth and nucleation rates as a function of time.

Analysis of the SAXS patterns recorded during the nanosphere synthesis with [OY] = 100 mM

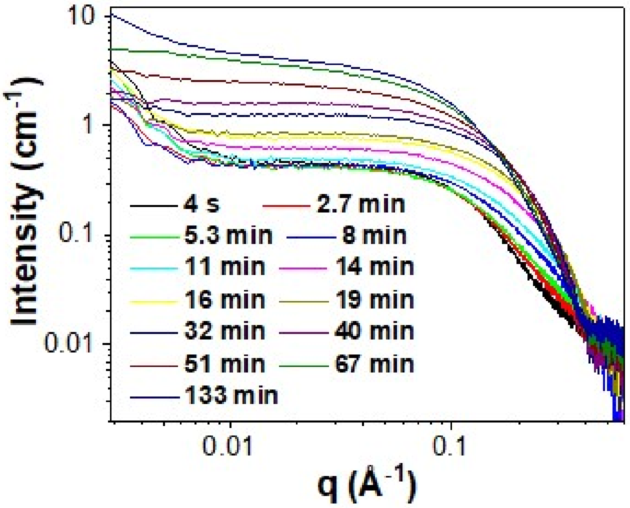

Figure S12. *In situ* time-resolved i*n situ* SAXS patterns recorded during the synthesis of Au nanoparticles with [OY] = 100 mM

Table S6. Structural fit parameters of SAXS signals during the induction and the growth stages of the synthesis of gold nanospheres using [OY] = 100 mM, using Beaucage model (Eq. S1). R_g is the gyration radius, D_{SAXS} the diameter of the objects calculated from the gyration radius assuming a spherical shape, p_1 refers to the slope of the Porod region.

Time	Pre-nucleation clusters Induction stage			
	R_g(Å)	D_{SAXS} (nm)	P_1	
0 s	15.1	3.9	3.1	
4 s	14.3	3.7	3.2	
2.7 min	12.8	3.3	3.1	
5.3 min	12.7	3.3	3.2	
Time	**Metal Nanoparticles Growth stage**			**Volume fraction PNCs/intermediate**
	R_g(Å)	D_{SAXS} (nm)	P_1	α_{PNCs}
11 min	7.4	1.9	4	0.95
14 min	7.6	2.0	4	0.83
16 min	8.4	2.2	4	0.76
19 min	8.7	2.3	4	0.69